Torsional wave propagation in a pre-stressed hyperelastic annular circular cylinder

Shearer, Tom and Abrahams, I. David and Parnell, William J. and Daros, Carlos H.

2013

MIMS EPrint: **2014.62**

Manchester Institute for Mathematical Sciences
School of Mathematics

The University of Manchester

Reports available from: http://eprints.maths.manchester.ac.uk/
And by contacting: The MIMS Secretary
School of Mathematics
The University of Manchester
Manchester, M13 9PL, UK

ISSN 1749-9097

TORSIONAL WAVE PROPAGATION IN A PRE-STRESSED HYPERELASTIC ANNULAR CIRCULAR CYLINDER

by TOM SHEARER[†], I. DAVID ABRAHAMS, WILLIAM J. PARNELL

(*School of Mathematics, University of Manchester, Manchester* M13 9PL)

and

CARLOS H. DAROS

(*Mechanical Engineering Faculty–FEM, State University of Campinas,* 13.083-970*, Campinas–SP, Brazil*)

[Received 25 February 2013. Revise 21 June 2013. Accepted 11 July 2013]

Summary

We consider torsional wave propagation in a pre-stressed annular cylinder. Hydrostatic pressure is applied to the inner and outer surfaces of an incompressible hyperelastic annular cylinder, of circular cross-section, whose constitutive behaviour is governed by a Mooney–Rivlin strain energy function. The pressure difference creates an inhomogeneous deformation field, which modifies the inner and outer radii of the annular cylinder. We wish to determine the effect that this pre-stress, and a given axial stretch, has on the propagation of small-amplitude torsional waves through the medium. We use the theory of small-on-large to deduce the linear wave equation that governs incremental torsional waves and then determine the dispersion relation for the pre-stressed annulus by using an approximation procedure (the Liouville–Green transformation). We show that this scheme compares well to numerical solutions except in regions very close to turning points (of the transformed ordinary differential equation). In particular, we find that the inhomogeneous deformation makes the coefficients of the governing ordinary differential equation spatially dependent and affects the location of the roots of the dispersion relation. We observe that, if the pressure on the outer surface of the annular cylinder is greater (smaller) than that on the inner, then the cut-on frequencies are spaced further apart (closer) than they would be in the stress-free case. This result could potentially be used to tune the propagation characteristics of the cylinder over a range of frequencies.

1. Introduction

Over the past few decades, much interest has been focused on the effect of pre-stress on the propagation of incremental linear waves in elastic media using the theory of *small-on-large* (**1**, **2**), where a small perturbation is applied to a body that has undergone a finite deformation. Since the perturbation is considered to be small in relation to the initial deformation, a linearization is applied in order to determine the characteristics of wave propagation in the pre-stressed material. Attention has centred mainly on the effect of *homogeneous* deformation on wave propagation, which induces anisotropy (examples of this are given in (**3**) and (**4**)). However, pre-stress in an *inhomogeneous* material almost always leads to inhomogeneous deformations, except in special cases (see (**5**), where the deformation of a one-dimensional composite bar is assumed to be piecewise homogeneous).

[†]<tom.shearer@postgrad.manchester.ac.uk>

Q. Jl Mech. Appl. Math, Vol. 66. No. 4 © The Author, 2013. Published by Oxford University Press;

Advance Access publication 24 October 2013. doi:10.1093/qjmam/hbt014

Dey (**6**) analysed the case of initial tension in a solid rod of circular cross-section in the context of linear elasticity. The interest was to determine how the presence of the tension affects the subsequent propagation of torsional waves through the material. This work utilized the incremental deformation theory derived by Biot (**7**). We emphasize that the pre-stress was homogeneous in this case, which meant that the incremental equations were straightforward to solve. Of great interest, however, is how an initial inhomogeneous pre-stress affects subsequent waves that propagate through inhomogeneous media. To address this question, by way of specific example, we consider herein the non-linear deformation of a cylindrical annulus and show that, for torsional waves, such a deformation leads to a governing ordinary differential equation (ODE) whose coefficients are spatially dependent. Non-linear pre-stress can be useful in practice, allowing us to *tune* materials in order to permit or restrict waves of specific frequency ranges. Parnell described this property in (**5**) and it is discussed further in subsequent articles in different contexts (**8**, **9**). The problem discussed here has potential applications in the automotive industry and also in the underwater engineering community.

Torsional wave propagation in the linear elastic (unstressed) regime is well understood (**10**). However, if the host material is non-linear-elastic (rubber, for example) we can expect pressures applied to the surfaces of an annular cylinder to lead to a non-linear deformation if such pressures are of the magnitude of the shear modulus of the material; hence we can postulate the following question: How does the difference in pressure on the surfaces of a hyperelastic annular cylinder affect the propagation of subsequent linear elastic torsional waves? In this article we shall consider a torsional wave propagating in an annular cylinder that is incompressible and capable of finite deformation, with constitutive behaviour characterized by a Mooney–Rivlin strain energy function. A related initial value problem in the case of zero pre-stress is discussed in (**11**), and for a solid cylinder on pp. 148–155 of (**10**). In (**12**) Green considered the effect of a uniform extension on torsional vibrations of a solid circular cylinder characterized by a general strain energy function, in which thermal stresses were taken into account and showed that they were possible under isothermal conditions, and in (**13**), Guz extended Green's work to the case where the cylinder was placed in a viscous fluid. In (**14**), Belward and Wright discussed the effect of a homogeneous axial stretch on the dispersion curves of small-amplitude waves having real frequencies and complex wavenumbers, and in (**15**), Ozturk and Akbarov considered torsional wave propagation in a prestretched compound hollow circular cylinder. However, in (**12–14**) and (**15**), the pre-stress was assumed to be uniform, that is, the stress distributions in the host materials were homogeneous. These are therefore far simpler problems than the model to be discussed in this article, since the only effect of their imposed pre-stress is to induce anisotropy in the media under consideration.

To the authors' knowledge, the only other investigation of the effect of inhomogeneous pre-stress on the propagation of torsional waves along an annular cylinder was performed by Engin and Şuhubi (**16**). These authors considered ostensibly the same problem as is discussed here (although in the absence of an axial stretch), utilizing Frobenius' method and a variational approach to study the effect of the pre-stress on the dispersion relations, and calculated the fundamental mode for various values of the pressure difference. However, in (**16**), an unphysical boundary condition was used, leading to results that are not in agreement to those found herein; this discrepancy is discussed in Section 4.2 and Appendix A.

In Section 2, we use the condition of incompressibility to determine the form of the applied radial deformation. The static equations of equilibrium are obtained and they are used to determine the effect of the applied pressures and longitudinal stretch on the radii. In Section 3 we consider the propagation of small-amplitude, time-harmonic waves through the finitely-deformed medium, derive the relevant governing equation and discuss the case of zero pre-stress. In Section 3.3 we discuss

the governing ODE, which is difficult to solve due to the spatial dependence of its coefficients, as mentioned above, and in Section 3.4 we derive an approximate solution for the ODE using the Liouville–Green method. In Section 4, we show the effect of the pre-stress on the dispersion curves using both a numerical method and the Liouville–Green approximation.

2. Initial finite (static) deformation

Here we consider the combined extension and inflation of an *incompressible*, annular cylinder with circular cross-section and initial inner and outer radii A and B, respectively. This problem can be found in several textbooks (**1**, **2**) but we present it here in a notation consistent with the rest of this article. We will assume that the annular cylinder is isotropic and that its constitutive behaviour may be described by a strain energy function, $W = W(I_1, I_2, I_3)$, where I_j are the principal strain invariants of the deformation (**1**, **2**). Since it is incompressible, $I_3 = 1$, in the usual notation, and thus $W = W(I_1, I_2)$. We suppose that radial pressures are applied on the inner and outer radii of the cylinder (which would occur, for example, if the cylinder were immersed in an inviscid fluid) so that under such loading the inner and outer radii are deformed to a and b, respectively. We also assume a constant axial stretch.

Due to the geometry there must be no displacement in the azimuthal direction, and so the above deformation can be described by

$$R = R(r), \quad \Theta = \theta, \quad Z = z/\lambda, \tag{2.1}$$

in which (R, Θ, Z) and (r, θ, z) are cylindrical polar coordinates in the undeformed and deformed configurations respectively, $R(r)$ is a function to be determined from the radial equation of equilibrium, and λ is a real constant representing the axial stretch. Note the convention introduced in (2.1) above, namely, upper case variables correspond to the undeformed configuration whilst lower case corresponds to the deformed configuration. Here, it will be convenient for us to derive equations in terms of coordinates in the deformed configuration, hence the form assumed in (2.1).

Position vectors in the undeformed and deformed configurations are

$$\boldsymbol{X} = \begin{pmatrix} R\cos\Theta \\ R\sin\Theta \\ Z \end{pmatrix} = \begin{pmatrix} R(r)\cos\theta \\ R(r)\sin\theta \\ z/\lambda \end{pmatrix}, \quad \boldsymbol{x} = \begin{pmatrix} r\cos\theta \\ r\sin\theta \\ z \end{pmatrix}. \tag{2.2}$$

Using (2.1), it can be shown that the principal stretches for this deformation in the radial, azimuthal and longitudinal directions are respectively

$$\lambda_r = \frac{dr}{dR} = \frac{1}{R'(r)}, \quad \lambda_\theta = \frac{r}{R} = \frac{r}{R(r)}, \quad \lambda_z = \lambda, \tag{2.3}$$

where prime denotes differentiation with respect to r. We define the deformation gradient tensor by $\boldsymbol{F} = \operatorname{Grad}\boldsymbol{x}$, where Grad represents the gradient operator with respect to the undeformed configuration. In our case, we have

$$\boldsymbol{F} = \begin{pmatrix} \lambda_r & 0 & 0 \\ 0 & \lambda_\theta & 0 \\ 0 & 0 & \lambda_z \end{pmatrix} = \begin{pmatrix} 1/R'(r) & 0 & 0 \\ 0 & r/R(r) & 0 \\ 0 & 0 & \lambda \end{pmatrix}. \tag{2.4}$$

For an incompressible material, we must have $J = \det \boldsymbol{F} = 1$, and so

$$\lambda_r \lambda_\theta \lambda_z = \frac{\lambda r}{R(r)R'(r)} = 1, \tag{2.5}$$

which is an ordinary differential equation that we can solve simply to obtain

$$R(r) = \sqrt{\lambda(r^2 + \alpha)}, \tag{2.6}$$

where α is a constant defined by

$$\alpha = \frac{A^2}{\lambda} - a^2 = \frac{B^2}{\lambda} - b^2. \tag{2.7}$$

Note that (2.6) gives the same form for R as in (**17**) (α is equivalent to M in (**17**)).

From (**18**), the Cauchy stress tensor for an incompressible material is given by

$$\boldsymbol{T} = \boldsymbol{F}\frac{\partial W}{\partial \boldsymbol{F}} + Q\boldsymbol{I}, \tag{2.8}$$

where W is the strain energy function of the material under consideration, $\boldsymbol{I}$ is the identity tensor and Q is a Lagrange multiplier associated with the incompressibility constraint and referred to as an *arbitrary hydrostatic pressure*. As mentioned in Section 1, we use the Mooney–Rivlin strain energy function:

$$W = \frac{\mu}{2}(S_1(I_1 - 3) + S_2(I_2 - 3)) = \frac{\mu}{2}(S_1(\lambda_r^2 + \lambda_\theta^2 + \lambda_z^2 - 3) + S_2(\lambda_r^2\lambda_\theta^2 + \lambda_r^2\lambda_z^2 + \lambda_\theta^2\lambda_z^2 - 3)). \tag{2.9}$$

Here, μ is the ground state shear modulus of the material under consideration, and S_1 and S_2 are two material parameters that sum to one.

Componentwise, (2.8) is equivalent to

$$T_{ij} = F_{i\alpha}\frac{\partial W}{\partial F_{j\alpha}} + Q\delta_{ij}, \tag{2.10}$$

where δ_{ij} is the Kronecker delta. We note that since $\boldsymbol{F}$ is diagonal in the cylindrical coordinate system we are using, so is $\boldsymbol{T}$ and therefore for the strain energy function in (2.9) we find that

$$\begin{aligned} T_{rr} &= \left[\chi S_1 + \left(\frac{1}{\lambda} + \lambda^2\chi\right)S_2\right]\frac{\mu}{\lambda} + Q, \\ T_{\theta\theta} &= \left[\frac{S_1}{\chi} + \left(\frac{1}{\lambda} + \frac{\lambda^2}{\chi}\right)S_2\right]\frac{\mu}{\lambda} + Q, \\ T_{zz} &= \left[\lambda S_1 + \left(2 + \frac{\alpha^2}{r^4\chi}\right)S_2\right]\lambda\mu + Q. \end{aligned} \tag{2.11}$$

where for convenience we have defined $\chi = \chi(r) = (r^2 + \alpha)/r^2$.

In the case considered here, the static equations of equilibrium, div $\boldsymbol{T} = \boldsymbol{0}$ (where div signifies the divergence operator with respect to the deformed configuration), reduce to

$$\frac{\partial T_{rr}}{\partial r} + \frac{1}{r}(T_{rr} - T_{\theta\theta}) = 0, \quad \frac{\partial T_{\theta\theta}}{\partial \theta} = 0, \quad \frac{\partial T_{zz}}{\partial z} = 0, \tag{2.12}$$

which then become

$$\frac{\partial Q}{\partial r} = \frac{\mu\alpha^2 S}{r^3(\alpha + r^2)}, \quad \frac{\partial Q}{\partial \theta} = \frac{\partial Q}{\partial z} = 0, \tag{2.13}$$

where we have defined $S = S_1/\lambda + \lambda S_2$. Therefore, Q depends only on r and can be expressed as

$$Q = -\frac{\mu S}{2}\left(\log\left(\frac{r^2}{r^2+\alpha}\right) + \frac{\alpha}{r^2}\right) + Q_0, \tag{2.14}$$

where Q_0 is a constant that can be deduced from the boundary conditions. This result can be used in (2.11) to determine explicit expressions for the stresses T_{rr}, $T_{\theta\theta}$ and T_{zz}.

If we label the hydrostatic pressures applied to the inner and outer surfaces of the annulus, respectively, as p_{in} and p_{out}, then, upon applying the boundary conditions $T_{rr}|_{r=a} = -p_{\text{in}}$ and $T_{rr}|_{r=b} = -p_{\text{out}}$, and rewriting the result in terms of the undeformed radii A and B and the parameter α, we find that

$$p_{\text{out}} - p_{\text{in}} = \mu S\left(\frac{(B^2 - A^2)\alpha}{2(A^2 - \lambda\alpha)(B^2 - \lambda\alpha)} + \log\left(\frac{A}{B}\sqrt{\frac{B^2 - \lambda\alpha}{A^2 - \lambda\alpha}}\right)\right). \tag{2.15}$$

Therefore, if we know the undeformed radii A and B, the applied pressure difference $p_{\text{out}} - p_{\text{in}}$, the material constants μ, S_1 and S_2, and the applied stretch λ, (2.15) can be used to determine the value of α, which can in turn be used to determine the deformed radii a and b from (2.7).

3. Incremental deformations

We now consider the propagation of small-amplitude time-harmonic waves through the finitely deformed medium. We use the theory of small-on-large, linearizing about a non-linear deformation state (**2**). The total displacement field may be represented by

$$\overline{\boldsymbol{U}} = \boldsymbol{U} + \boldsymbol{u}. \tag{3.1}$$

where $\boldsymbol{U}$ is the displacement field derived from the finite deformation (2.1) and $\boldsymbol{u}$ is the incremental displacement. Here, we take the incremental displacement in the form of a torsional wave:

$$\boldsymbol{u} = \text{Re}\left\{(0, v(r), 0)e^{i(kz-\omega t)}\right\}, \tag{3.2}$$

and assume that $|\boldsymbol{u}| \ll |\boldsymbol{U}|$.

In Appendix A, we show that the incremental equation governing v is

$$\left(1+\frac{\alpha}{r^2}\right)v''(r)+\frac{1}{r}\left(1-\frac{\alpha}{r^2}\right)v'(r)+\left(\beta^2-\frac{1+\alpha\delta}{r^2}+\frac{\alpha}{r^4}\right)v(r)=0, \tag{3.3}$$

where

$$\beta^2=\frac{k_0^2-k^2\lambda^2S_1}{S}-\delta, \quad \delta=\frac{k^2\lambda S_2}{S}, \tag{3.4}$$

in which $k_0^2=\rho\omega^2/\mu$ is the zeroth order torsional wavenumber of an unstressed cylinder, ρ represents the mass density, α is defined in (2.7) and we recall that $S=S_1/\lambda+\lambda S_2$.

If we assume that the pressures on the deformed surfaces of the annulus are unaffected by the incremental deformation then (3.3) is subject to the boundary conditions (derived in Appendix A)

$$v'(a)-\frac{v(a)}{a}=v'(b)-\frac{v(b)}{b}=0. \tag{3.5}$$

We note that these boundary conditions are different to those derived in (**16**), as we discuss in Appendix A.

3.1 *The case of zero pre-stress*

To study the effects of pre-stress it is first useful to examine torsional waves in the absence of such static loads. Zero pre-stress corresponds to the situation when $\alpha=0$ and $\lambda=1$ and in this case (3.3) reduces to

$$v''(r)+\frac{1}{r}v'(r)+\left(\frac{\omega^2}{c^2}-k^2-\frac{1}{r^2}\right)v(r)=0, \tag{3.6}$$

where $c^2=\mu/\rho$. This is Bessel's equation and is the standard *linear* elastic torsional wave equation (**10**). The solution of (3.6) is thus

$$v(r)=C_1\mathrm{J}_1(sr)+C_2\mathrm{Y}_1(sr), \tag{3.7}$$

where J_1 and Y_1 are the first-order Bessel functions of the first and second kind respectively and $s^2=\omega^2/c^2-k^2$. Imposing the conditions (3.5), we obtain the classical dispersion relation

$$\frac{as\mathrm{J}_0(as)-2\mathrm{J}_1(as)}{bs\mathrm{J}_0(bs)-2\mathrm{J}_1(bs)}=\frac{as\mathrm{Y}_0(as)-2\mathrm{Y}_1(as)}{bs\mathrm{Y}_0(bs)-2\mathrm{Y}_1(bs)}. \tag{3.8}$$

This dispersion relation leads to the well-known result that a thicker cylindrical annulus (smaller value of a/b, with $a=0$ in the solid cylinder limit) will allow more modes of propagation for a given fixed frequency than a thin annular cylinder. Our main interest here is how this dispersion relation is modified by the non-linear elastic pre-stress and its dependence on the Mooney–Rivlin strain energy function parameter $S_1=1-S_2$. In Fig. 1, we plot the frequencies of the first, second and third roots of (3.8) as a function of annulus thickness, a/b, with $b=1$. We note that $\omega/c\to\infty$ as $a/b\to 0$. This is due to the fact that no torsional modes propagate in an infinitesimally thin cylindrical annulus.

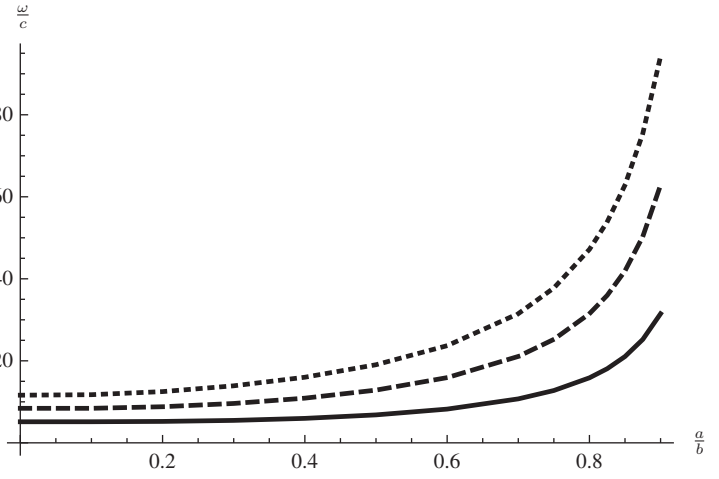

Fig. 1 The first (solid), second (dashed) and third (dotted) cut-on frequencies of (3.8) as a function of a/b

3.2 *Analytical solution in the case of* $\omega = k = 0$

It is useful to examine the case when $\omega = k = 0$, to see if the boundary value problem has a consistent solution. The governing ODE (3.3) reduces to

$$\left(1 + \frac{\alpha}{r^2}\right) v''(r) + \frac{1}{r}\left(1 - \frac{\alpha}{r^2}\right) v'(r) - \frac{1}{r^2}\left(1 - \frac{\alpha}{r^2}\right) v(r) = 0, \tag{3.9}$$

for which an analytical solution can be found as

$$v(r) = C_1 r + C_2 r \log\left(\frac{r^2}{r^2 + \alpha}\right), \tag{3.10}$$

where C_1 and C_2 are arbitrary constants.

Applying the boundary conditions (3.5) gives $C_2 = 0$ and C_1 is unspecified. This shows that for any magnitude of pre-stress, there will always be a non-trivial solution with $\omega = k = 0$; hence the fundamental mode will always pass through the origin when the dispersion curves are plotted, as we will see later.

3.3 *Non-zero pre-stress: singularity structure*

Note that in the case of non-zero pre-stress the governing equation (3.3) has regular singular points at $r = 0$, $r = \sqrt{\alpha}i$ and $r = -\sqrt{\alpha}i$ and an irregular singular point at $r = \infty$. All other points are ordinary points. To the authors' knowledge (3.3) is not a standard and classified ODE,[1] so we will investigate

[1] However, we thank the editor for pointing out that (3.3) can be rewritten as a confluent form of Heun's equation (see §31.2(ii) of (**19**)).

the solution. Note that it is difficult to solve due to the spatial dependence of its coefficients and the singular nature of the zero pre-stress limit.

The Frobenius method can be used to determine an approximate solution in the case when $a, b < \sqrt{|\alpha|}$ or $a, b > \sqrt{|\alpha|}$ in terms of an infinite series and these cases are considered in (**16**). However, when $a \leq \sqrt{\alpha}$ and $b \geq \sqrt{\alpha}$, the singularity will always lie within the annulus and so the Frobenius method breaks down. Since we are interested in this possibility, in the following section we present a Liouville–Green approximate solution of the ODE.

3.4 *Liouville–Green solution*

Let us restate the original ODE for incremental waves:

$$\left(1+\frac{\alpha}{r^2}\right)v''(r)+\frac{1}{r}\left(1-\frac{\alpha}{r^2}\right)v'(r)+\left(\beta^2-\frac{1+\alpha\delta}{r^2}+\frac{\alpha}{r^4}\right)v(r)=0. \tag{3.11}$$

First divide (3.11) by the term multiplying the highest derivative so that it can be written as

$$v''(r)+P(r)v'(r)+Q(r)v(r)=0, \tag{3.12}$$

with $P(r)$ and $Q(r)$ defined as

$$P(r)=\frac{1}{r}\frac{r^2-\alpha}{r^2+\alpha}, \quad Q(r)=\frac{1}{r^2+\alpha}\left(r^2\beta^2-(1+\alpha\delta)+\frac{\alpha}{r^2}\right). \tag{3.13}$$

We can now eliminate the first derivative in (3.12) using a standard transformation of the dependent variable v (**20**),

$$v(r)=w(r)e^{-\frac{1}{2}\int P(r)\,dr}, \tag{3.14}$$

so that (3.12) is transformed into the following ODE

$$w''(r)+q(r)w(r)=0. \tag{3.15}$$

Here the polynomial quotient function $q(r)$ is defined as

$$q(r)=\frac{\hat{q}(\hat{r})}{b^2}, \tag{3.16}$$

where

$$\hat{q}(\hat{r})=\frac{4\hat{\beta}^2\hat{r}^6+(4\hat{\alpha}(\hat{\beta}^2-\hat{\delta})-3)\hat{r}^4-2\hat{\alpha}(2\hat{\alpha}\hat{\delta}+3)\hat{r}^2+\hat{\alpha}^2}{4\hat{r}^2(\hat{r}^2+\hat{\alpha})^2}, \quad \hat{r}=\frac{r}{b}, \tag{3.17}$$

$$\hat{\alpha}=\frac{\alpha}{b^2}=\frac{1}{\lambda}\left(\frac{B}{b}\right)^2-1, \quad \hat{\beta}^2=b^2\beta^2=\frac{\hat{k}_0^2-\hat{k}^2\lambda^2S_1}{S}-\hat{\delta}, \quad \hat{\delta}=b^2\delta=\frac{\hat{k}^2\lambda S_2}{S}, \tag{3.18}$$

and

$$\hat{k}_0^2=b^2k_0^2, \quad \hat{k}^2=b^2k^2. \tag{3.19}$$

Note that we have introduced the hat notation $\hat{(\cdot)}$ to signify that the above variables are all non-dimensional.

Assuming for now that $q(r)$ is a positive and twice continuously differentiable function, we apply the Liouville–Green (LG) transformation (**20**) by defining

$$\xi(r) = \int^r \sqrt{q(\varrho)}\, d\varrho, \quad \mathcal{W}(\xi) = \{\xi'(r)\}^{\frac{1}{2}} w(r(\xi)). \tag{3.20}$$

Upon doing this we obtain the governing equation

$$\frac{d^2\mathcal{W}}{d\xi^2} + (1 - \varphi(\xi))\mathcal{W}(\xi) = 0, \tag{3.21}$$

where

$$\varphi(\xi(r)) = \psi(r) = \frac{4\,q(r)q''(r) - 5\,\left\{q'(r)\right\}^2}{16\,\{q(r)\}^3} = -\frac{1}{\{q(r)\}^{3/4}}\frac{d^2}{dr^2}\{q(r)\}^{-\frac{1}{4}}. \tag{3.22}$$

If the function φ is assumed small and hence can be neglected, then independent solutions of (3.21) are $e^{\pm i\,\xi}$. Restoring the original dependent (w) and independent (r) variables we obtain

$$w(r) = C_1\,(q(r))^{-\frac{1}{4}}\,e^{i\xi(r)} + C_2\,(q(r))^{-\frac{1}{4}}\,e^{-i\xi(r)}, \tag{3.23}$$

where C_1 and C_2 are constants of integration. Notice that the restriction $q(r) > 0$ ensures that the solutions (3.23) are wave-like. When $q(r)$ changes its sign in the interval of r under consideration, we have then what are conventionally called *turning points* or *transition points* of the ODE (zeros of q). In that case the appropriate approximation functions are the Airy (one turning point) or Weber parabolic cylinder functions (two turning points) (**20**). The error in this approximation is obviously dependent on the behaviour of the neglected function $\varphi(\xi(r)) = \psi(r)$. If $\{q(r)\}^{-1/4}$ is small or slowly varying then we have a good approximation for the ODE. Finally, when $q(r)$ is positive and the interval under consideration is far from the turning point(s) it can be shown that the functions $e^{\pm i\xi}$ are suitable ones for the approximate solution of the ODE.

Our final step is to transform back to the original dependent variable v using the transformation (3.14):

$$v(r) = w(r)e^{-\frac{1}{2}\int P(\hat{r})\,dr} = w(r)e^{-\frac{1}{2}\log((\alpha+r^2)/r)}. \tag{3.24}$$

Upon doing this we obtain the final form of the approximate solution of the ODE

$$v(r) = C_1\,(q(r))^{-\frac{1}{4}}\,e^{i\xi(r)-\frac{1}{2}\log((\alpha+r^2)/r)} + C_2\,(q(r))^{-\frac{1}{4}}\,e^{-i\xi(r)-\frac{1}{2}\log((\alpha+r^2)/r)}. \tag{3.25}$$

Notice that the LG approximation implies the transformation of the independent variable r into $\xi(r)$, obtained via the integration of the square root of the function $q(r)$. For many problems, an explicit form for this integral is not generally available. However, in Appendix B we show that for the present problem this integral can be explicitly evaluated in terms of the three incomplete elliptic integrals and elementary functions; see (B.9).

In Figs 2 and 3 we give plots of the curves $\hat{q}(\hat{r}) = 0$ (and hence $q(r) = 0$) for specific values of $\hat{\alpha}$ and $\hat{\delta}$ (the regions below the curves are the regions where $\hat{q}(\hat{r})$ is negative). In the plots $\hat{r}$ ranges over the horizontal axis and $\hat{\beta}$ ranges over the vertical axis. We observe that increasing the value of $\hat{\alpha}$ improves the range over which the method is expected to work (for which $\hat{q}(\hat{r}) > 0$), whereas increasing $\hat{\delta}$ has the opposite effect. Increasing $|\hat{\alpha}|$ corresponds to increasing pre-stress,

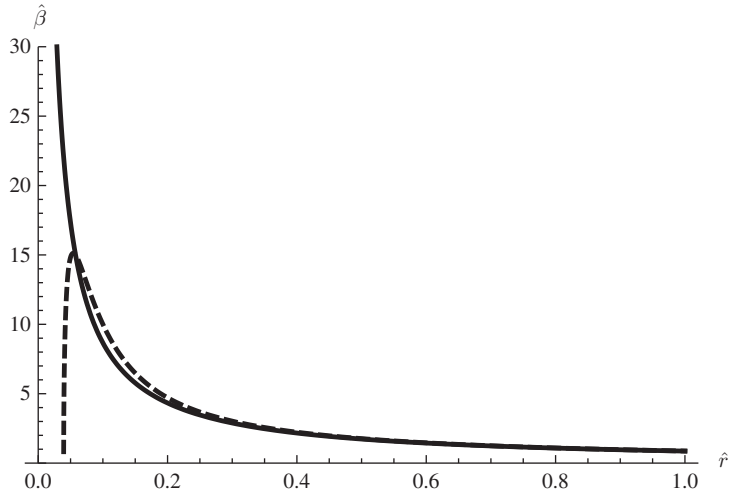

Fig. 2 Curves of $\hat{q}(\hat{r}) = 0$. Solid line: $\hat{\alpha} = 0$, $\hat{\delta} = 0$; dashed line: $\hat{\alpha} = 0.01$, $\hat{\delta} = 0$

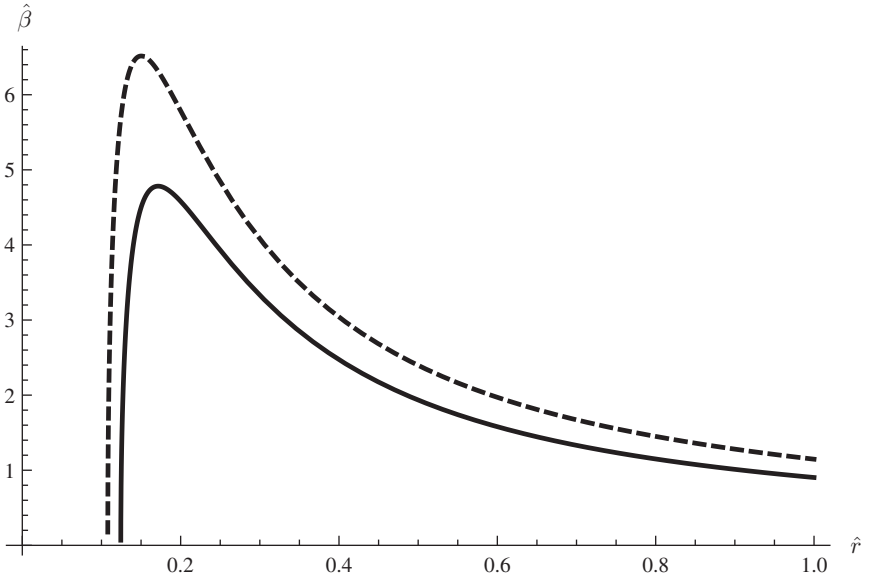

Fig. 3 Curves of $\hat{q}(\hat{r}) = 0$. Solid line: $\hat{\alpha} = 0.1$, $\hat{\delta} = 0$; dashed line: $\hat{\alpha} = 0.1$, $\hat{\delta} = 5$

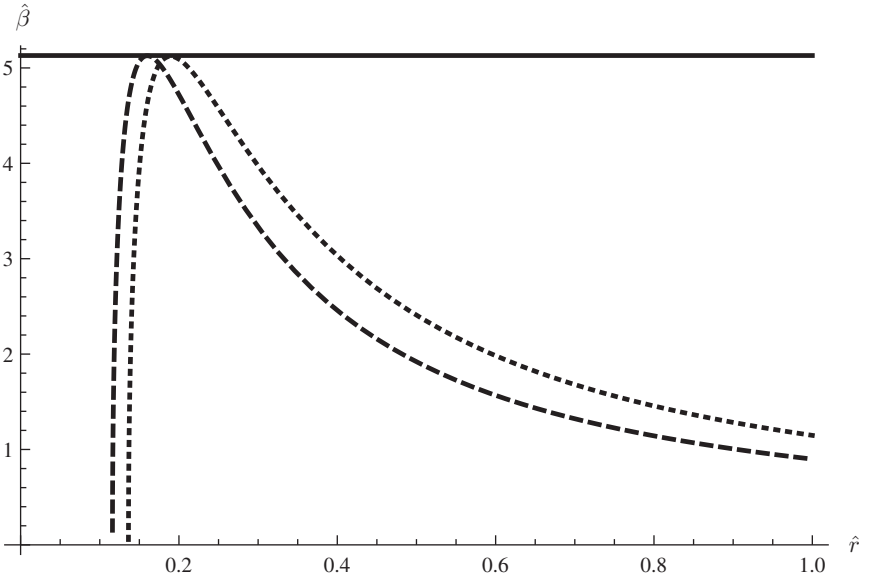

Fig. 4 Curves of $\hat{q}(\hat{r}) = 0$. Dashed line: $\hat{\alpha} = 0.087$, $\hat{\delta} = 0$; dotted line: $\hat{\alpha} = 0.157$, $\hat{\delta} = 3$. The solid line is $\hat{\beta} = 5.14$, the smallest non-zero value $\hat{\beta}$ can take for a stress-free annular cylinder

$\hat{\alpha} > 0$ corresponds to $p_{\text{out}} > p_{\text{in}}$ and $\hat{\alpha} < 0$ corresponds to $p_{\text{out}} < p_{\text{in}}$. Increasing $\hat{\delta}$ corresponds to increasing dependence of the particular strain energy function on the parameter S_2.

We know that, for a stress-free annular cylinder with $a = 0$ (the solid cylinder limit), the smallest non-zero value $\hat{\beta}$ can take is approximately 5.14. Increasing the inner radius from 0 increases the smallest non-zero value of $\hat{\beta}$ (see Fig. 1 and note that in this figure, increasing ω/c corresponds to increasing $\hat{\beta}$). We have also shown that increasing the value of $\hat{\alpha}$ improves the range of validity of the LG method. Therefore, in Fig. 4 we show that for $\hat{\alpha}$ greater than approximately 0.087 the LG method should work for all neo-Hookean annular cylinders. However, for a greater value of $\hat{\delta}$ this critical value of $\hat{\alpha}$ is increased. Note that Fig. 6 reveals that, for negative pressures, the distance to the first non-zero root of the dispersion curves decreases slowly, and so we expect that the region where the LG method is inaccurate increases slowly too.

4. Dispersion curves: predictions via numerical and Liouville–Green solutions

4.1 *Neo-Hookean case*

In the neo-Hookean case, we have $S_2 = 0$ and therefore $\delta = 0$, so the dispersion relations can be determined simply by determining the values of β which satisfy the boundary conditions. Using a standard numerical solver one can obtain an interpolating polynomial solution for $v(r)$ for particular values of a and b. The numerical solver used in this article was *NDSolve* in *Mathematica 8*. Alternatively, the LG solution (Section 3.4) can be used. Either method can be employed to find values of β^2 which satisfy the boundary conditions, and hence define the dispersion curves for the problem.

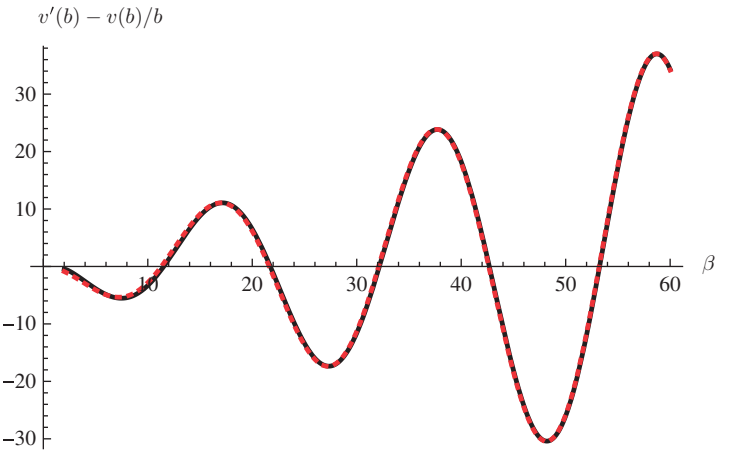

Fig. 5 Prediction of cut-on frequencies using Liouville–Green method (solid) and a numerical solver (dashed) for $a = 0.5$, $b = 1$, $S_2 = 0$, $\alpha = 1$

For both methods, we apply the boundary condition derived in Appendix A.2 on $r = a$, and also arbitrarily choose the torsional wave eigensolution to have amplitude $v(a) = 1$. We then plot $v'(b) - v(b)/b$ as a function of β in order to determine the values of β which correspond to the cut-on frequencies for the problem (that is, when this function vanishes). In Fig. 5 we plot $v'(b) - v(b)/b$ as a function of β for $a = 0.5$, $b = 1$, $S_2 = 0$, $\alpha = 1$. Note that, as expected, the agreement is better for larger values of β.

We note that the numerical solver always predicts $\beta = 0$ as a root, which is the fundamental mode. In this case we have $k_0^2 - k^2\lambda(\lambda S_1 + S_2) = 0$, and hence

$$k^2 = \frac{k_0^2}{\lambda(\lambda S_1 + S_2)}. \tag{4.1}$$

We observe from (4.1) that the only modification to the fundamental mode is a change in gradient, which is dependent on the longitudinal stretch factor, λ, and S_1 or S_2.

By plotting the dispersion curves for various values of a, b, λ and α, it can be observed that a positive value of α (which corresponds to $p_{\text{in}} > p_{\text{out}}$) causes the roots of the dispersion curves to be spaced further apart, whilst a negative value of α (which corresponds to $p_{\text{in}} < p_{\text{out}}$) causes them to be spaced more closely. It can also be observed that for $\lambda > 1$ (corresponding to a longitudinal stretch), the cut-on frequencies are closer together and the dispersion curves are less steep, whilst for $\lambda < 1$ (corresponding to a longitudinal compression) the cut-on frequencies are spaced further apart and the dispersion curves are steeper.

In Fig. 6, we show the first three cut-on frequencies as a function of $(p_{\text{out}} - p_{\text{in}})/(S\mu)$ for a neo-Hookean ($S_1 = 1$, $S_2 = 0$) annular cylinder with $a = 0.5$ and $b = 1$ using the numerical solution. In Fig. 7, we do the same with $A = 0.5$ and $B = 1$. In Fig. 8 we give the dispersion curves for a neo-Hookean ($S_1 = 1$, $S_2 = 0$) annular cylinder with $a = 0.5$ and $b = 1$, with $\lambda = 1$ and $(p_{\text{out}} - p_{\text{in}})/(S\mu) = 0$, 1.96, and 3.55. In Fig. 9 we give the same, but for $A = 0.5$ and $B = 1$. Note that Figs 8 and 9 were produced using a numerical solver rather than the LG method.

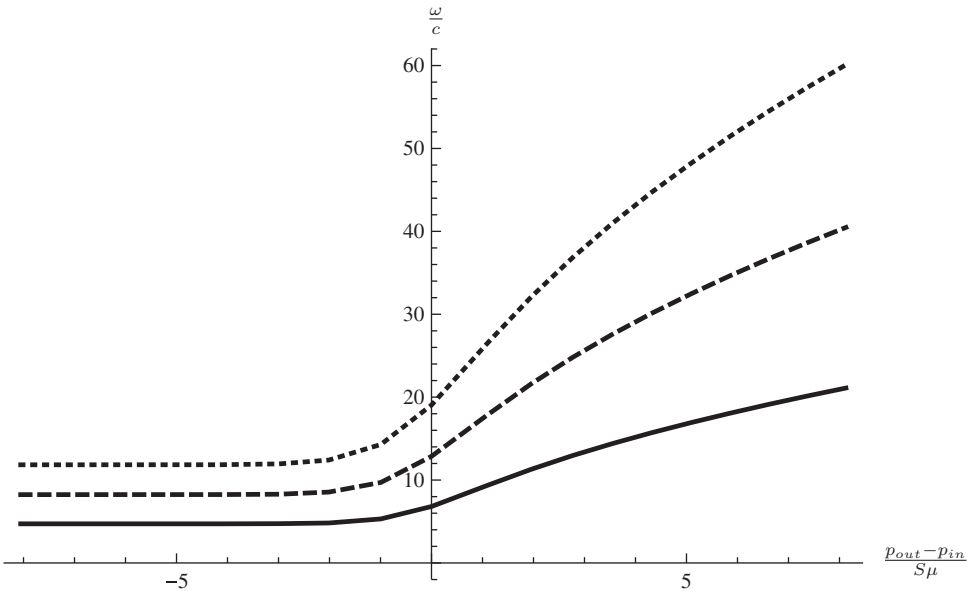

Fig. 6 First (solid), second (dashed) and third (dotted) cut-on frequencies for a pre-stressed neo-Hookean ($S_1 = 1, S_2 = 0$) cylinder as a function of $(p_{\text{out}} - p_{\text{in}})/(S\mu)$ with $a = 0.5$ and $b = 1$

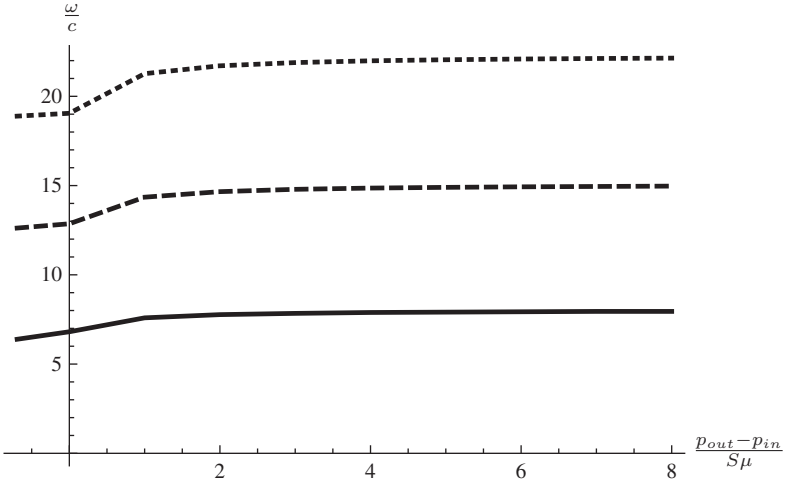

Fig. 7 First (solid), second (dashed) and third (dotted) cut-on frequencies for a pre-stressed neo-Hookean ($S_1 = 1, S_2 = 0$) cylinder as a function of $(p_{\text{out}} - p_{\text{in}})/(S\mu)$ with $A = 0.5$ and $B = 1$

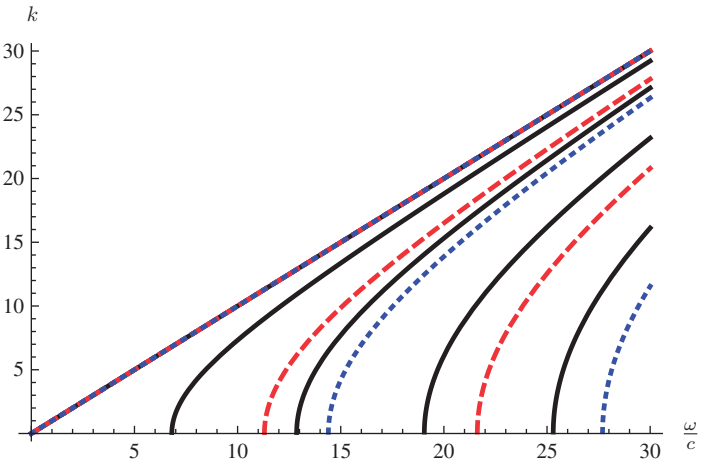

Fig. 8 Dispersion curves for a neo-Hookean ($S_1 = 1,\ S_2 = 0$) annular cylinder of *deformed* inner radius 0.5 and outer radius 1, with $\lambda = 1$ and $(p_{\text{out}} - p_{\text{in}})/(S\mu) = 0$ (solid), 1.96 (dashed) and 3.55 (dotted)

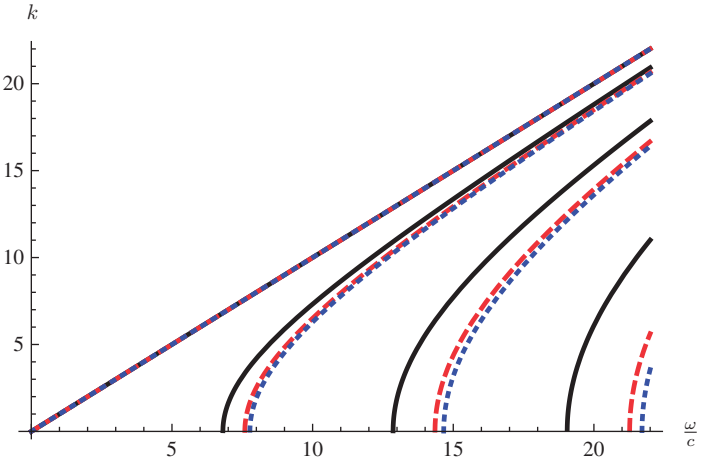

Fig. 9 Dispersion curves for a neo-Hookean ($S_1 = 1,\ S_2 = 0$) annular cylinder of *initial* inner radius 0.5 and outer radius 1, with $\lambda = 1$ and $(p_{\text{out}} - p_{\text{in}})/(S\mu) = 0$ (solid), 1.96 (dashed) and 3.55 (dotted)

4.2 *Mooney–Rivlin case*

In the Mooney–Rivlin case, $\delta \neq 0$, and so the dispersion relations cannot be determined by the value of β alone. In this case we evaluate the boundary condition $v'(b) - v(b)/b = 0$ as a two-dimensional function of k and $k_0 = \omega/c$ and plot the regions where this function equals zero. These plots are our dispersion curves. In Fig. 10 we plot the dispersion curves for a Mooney–Rivlin ($S_1 = 0.8,\ S_2 = 0.2$)

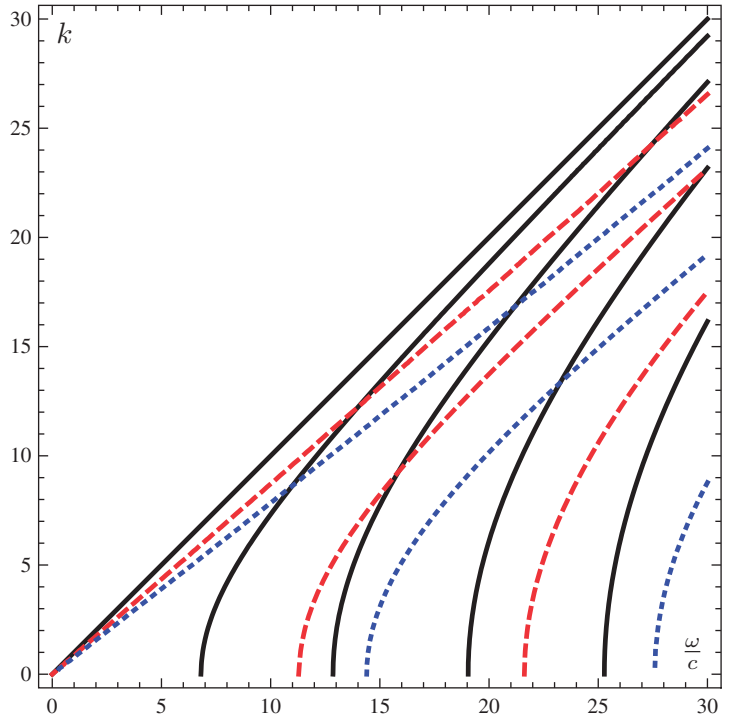

Fig. 10 Dispersion curves for a Mooney–Rivlin ($S_1 = 0.8,\ S_2 = 0.2$) annular cylinder of *deformed* inner radius 0.5 and outer radius 1, with $\lambda = 1$ and $(p_{\text{out}} - p_{\text{in}})/(S\mu) = 0$ (solid), 1.96 (dashed) and 3.55 (dotted)

annular clyinder with $a = 0.5$ and $b = 1$, with $\lambda = 1$ and $(p_{\text{out}} - p_{\text{in}})/(S\mu) = 0$, 1.96, and 3.55. Fig. 10 was produced using a numerical solver.

The trends observed in the Mooney–Rivlin case are the same as those in the neo-Hookean case except that in the latter case (when $S_1 = 1,\ S_2 = 0$), α does not affect the gradients of the dispersion curves, whereas in the Mooney–Rivlin case, a positive value of α decreases their gradients and a negative value increases them.

We note that the fundamental mode always passes through the point $(\omega/c, k) = (0, 0)$ and is always non-dispersive. This result corrects that of Engin and Şuhubi (**16**) where the fundamental mode was deduced to be dispersive due to the erroneous boundary conditions used.

5. Conclusion

In this article, we have studied the problem of torsional wave propagation in a pre-stressed Mooney–Rivlin hyperelastic annular cylinder. The pre-stress consists of a uniform longitudinal stretch and hydrostatic pressures imposed on the inner and outer surfaces of the cylinder, thus altering the radii. Importantly, the latter generates an inhomogeneous deformation in the cylinder.

The theory of small-on-large was used to derive the incremental equation in the pre-stressed configuration. It was shown that this equation was difficult to solve due to the spatial dependence of

its coefficients and the singular limit of the equation in the case of zero pre-stress. In Section 3.4, we presented a Liouville–Green approximation to the solution of the ODE and discussed when we expect this to be a good approximation. It was shown that for $\hat{\alpha} > 0.087$ we expect the LG approximation to be good for a neo-Hookean annular cylinder of any size, and this was confirmed by comparison with a numerical solution of the boundary value problem.

We noted that a positive value of α (which corresponds to $p_{\text{out}} > p_{\text{in}}$) causes the roots of the dispersion curves to be spaced further apart, whilst a negative value of α (corresponding to $p_{\text{out}} < p_{\text{in}}$) causes them to be spaced more closely. In the neo-Hookean case (when $S_1 = 1$, $S_2 = 0$), α does not affect the gradients of the dispersion curves, whereas in the Mooney–Rivlin case, a positive value of α decreases their gradients and a negative value increases them. We also noted that for $\lambda > 1$ (corresponding to a longitudinal stretch) the cut-on frequencies move closer together and the dispersion curves are less steep, whilst for $\lambda < 1$ (corresponding to a longitudinal compression) the cut-on frequencies move further apart and the dispersion curves are steeper.

In conclusion, we have conducted a small-on-large study into the effect of inhomogeneous pre-stress on torsional wave propagation. The dependence of the cut-on frequencies on the pre-stress could potentially be used to tune which modes are able to propagate over a given range of frequencies. For example, if it was required to reduce the number of torsional modes that propagate along an annular cylinder at a given frequency, we have demonstrated that applying a large enough pressure on the outer surface would achieve this. Potential areas of further work would be a study into the effect of the elastic parameter S_2 on the stated results, and an investigation of whether the behaviour of the cylinder would be similar for other choices of strain energy function.

References

1. A. E. Green and W. Zerna, *Theoretical Elasticity* (Dover, New York 1992).
2. R. W. Ogden, *Non-linear Elastic Deformations* (Dover, New York 1997).
3. M. Destrade and N. Scott, Surface waves in a deformed isotropic hyperelastic material subject to an isotropic internal constraint, *Wave Motion* **40** (2004) 347–357.
4. J. D. Kaplunov and G. A. Rogerson, An asymptotically consistent model for long-wave high frequency motion in a pre-stressed elastic plate, *Math. Mech. Solids* **7** (2002) 581–606.
5. W. J. Parnell, Effective wave propagation in a pre-stressed nonlinear elastic composite bar, *IMA J. Appl. Math.* **72** (2007) 223–244.
6. S. Dey, Torsional wave under initial stress. *Pure Appl. Geophys.* **94** (1972) 53–59.
7. M. A. Biot, *Mechanics of Incremental Deformation* (Wiley, New York 1965).
8. K. Bertoldi and M. C. Boyce, Wave propagation and instabilities in monolithic and periodically structured elastomeric materials undergoing large deformations, *Phys. Rev.* B **78** (2008), 184107.
9. M. Gei, A. B. Movchan and D. Bigoni, Band-gap shift and defect-induced annihilation in prestressed elastic structures, *J. Appl. Phys.* **105** (2009), 063507.
10. J. Billingham and A. C. King, *Wave Motion* (Cambridge University Press, Cambridge 2001).
11. A. Ertepinar and A. Gürkök, Free torsional oscillations of hollow circular cylinders made of a Mooney material, *J. Sound Vib.* **80** (1982) 305–313.
12. A. E. Green, Torsional vibrations of an initially stressed cylinder, *Problems of Continuum Mechanics* (Muskhelishvili Anniversary Volume), SIAM, Philadelphia, Pennsylvania, 1961, 148–154.

13. A. N. Guz, Aerohydroelastic problems for bodies with initial stresses, *Sov. Appl. Mech.* **16** (1980) 175–190.
14. J. A. Belward and S. J. Wright, Small-amplitude waves with complex wave numbers in a prestressed cylinder of Mooney material, *Quart. Jl Mech. Appl. Math.* **40** (1987) 383–399.
15. A. Ozturk and S. D. Akbarov, Propagation of torsional waves in a prestretched compound hollow circular cylinder, *Mech. Composite Materials* **44** (2008) 77–86.
16. H. Engin and E. S. Şuhubi, Torsional oscillations of an infinite cylindrical elastic tube under large internal and external pressure, *Int. J. Engng Sci.* **16** (1978) 387–396.
17. W. J. Parnell and I. D. Abrahams, Antiplane wave scattering from a cylindrical void in a pre-stressed incompressible neo-Hookean material, *Commun. Comp. Phys.* **11** (2012) 367–382.
18. M. Destrade and G. Saccomandi, *Waves in Nonlinear Pre-Stressed Materials* (Springer Wien, New York 2007).
19. *NIST Digital Library of Mathematical Functions*. http://dlmf.nist.gov/, Release 1.0.6 of 2013-05-06.
20. F. W. J. Olver, *Asymptotics and Special Functions* (Academic Press, New York 1974).

APPENDIX A

A. Incremental deformations

A.1 *Incremental equations of motion*

We consider a perturbation to the initial deformation in the form of a torsional wave and wish to determine the incremental equation governing this wave using the theory of small-on-large. We will use an adaptation of Ogden's notation, following the method outlined in (**2**) which we summarize below. We denote the incremental displacement by $\boldsymbol{u}$ and for torsional waves this takes the form

$$\boldsymbol{u} = (0, v(r)e^{ikz}, 0)e^{-i\omega t}, \tag{A.1}$$

and its gradient with respect to the deformed configuration is given by

$$\boldsymbol{\gamma} = \operatorname{grad} \boldsymbol{u} = \begin{pmatrix} 0 & -v/r & 0 \\ v'(r) & 0 & ikv \\ 0 & 0 & 0 \end{pmatrix} e^{i(kz-\omega t)}. \tag{A.2}$$

The push forward of the nominal stress for an incompressible material is given by

$$\boldsymbol{\zeta} = \boldsymbol{F}\boldsymbol{s} = \boldsymbol{M} : \boldsymbol{\gamma} + q\boldsymbol{I} - Q\boldsymbol{\gamma}, \tag{A.3}$$

where $\boldsymbol{s}$ is the incremental nominal stress tensor, and $\boldsymbol{M}$ is the push forward of the elasticity tensor defined by

$$M_{ijkl} = \frac{\partial^2 W}{\partial F_{jm} \partial F_{ln}} F_{im} F_{kn}, \tag{A.4}$$

often denoted by $\boldsymbol{\mathcal{A}_0}$ and q is the increment of Q. We will assume that $q = q(r, z)$ (that is, independent of θ since there is no θ dependence in either the pre-stress or the perturbation).

The incremental equations of motion are then given by

$$\operatorname{div} \boldsymbol{\zeta} = \rho \frac{\partial^2 \mathbf{u}}{\partial t^2}, \tag{A.5}$$

where ρ is the density of the body, which remains constant throughout the deformation, since we are considering an incompressible material.

Using (A.5), we observe that the radial and axial equations give respectively

$$\frac{\partial \zeta_{11}}{\partial r} = 0, \quad \frac{\partial \zeta_{33}}{\partial z} = 0, \tag{A.6}$$

and the azimuthal equation is given by

$$\frac{\partial \zeta_{12}}{\partial r} + \frac{\partial \zeta_{32}}{\partial z} + \frac{\zeta_{12} + \zeta_{21}}{r} = -\rho\omega^2 v(r) e^{i(kz-\omega t)}. \tag{A.7}$$

Now, from (**18**) we have $M_{iijj} = \lambda_i \lambda_j W_{ij}$, and, when $i \neq j$, $\lambda_i \neq \lambda_j$,

$$M_{ijij} = \frac{\lambda_i W_i - \lambda_j W_j}{\lambda_i^2 - \lambda_j^2} \lambda_i^2, \quad M_{ijji} = \frac{\lambda_j W_i - \lambda_i W_j}{\lambda_i^2 - \lambda_j^2} \lambda_i \lambda_j,$$

where

$$W_i = \frac{\partial W}{\partial \lambda_i}, \quad W_{ij} = \frac{\partial^2 W}{\partial \lambda_i \partial \lambda_j},$$

and we note that, in the above, there is no implied summation over repeated indices and, for all other combinations of i, j, k and l, we have $M_{ijkl} = 0$.

Therefore, using the Mooney–Rivlin strain energy function in (A.3), we have

$$\zeta_{11} = q, \quad \zeta_{22} = q, \quad \zeta_{33} = q, \tag{A.8}$$

$$\zeta_{12} = \left(\frac{S_2\mu + \lambda^2 Q}{\lambda^2 r} v(r) + \frac{1}{\lambda} \left(1 + \frac{\alpha}{r^2} \right) (S_1 + \lambda^2 S_2) \mu v'(r) \right) e^{i(kz-\omega t)}, \tag{A.9}$$

$$\zeta_{21} = -\left(\frac{(S_1 + \lambda^2 S_2)\mu r}{\lambda(\alpha + r^2)} v(r) + \frac{S_2\mu + \lambda^2 Q}{\lambda^2} v'(r) \right) e^{i(kz-\omega t)}, \tag{A.10}$$

$$\zeta_{23} = -ik \left(\frac{\lambda r^2 S_2 \mu}{\alpha + r^2} + Q \right) v(r) e^{i(kz-\omega t)}, \tag{A.11}$$

$$\zeta_{32} = ik\lambda \left(\frac{\alpha S_2}{r^2} + \lambda S_1 + S_2 \right) \mu v(r) e^{i(kz-\omega t)}, \tag{A.12}$$

which, referring to (A.7), leads to the governing equation for v, (3.3). Also (A.6) give

$$\frac{\partial q}{\partial r} = \frac{\partial q}{\partial z} = 0, \tag{A.13}$$

so that $q = q(r, z)$ must be a constant. The boundary conditions, to be discussed next, determine this constant.

A.2 *Boundary conditions*

We apply the condition that the perturbation $v(r)$ does not affect the pressure on the surfaces $r = a, b$ of the deformed annulus. For this to hold, we must have

$$\bar{\boldsymbol{T}}\bar{\boldsymbol{n}}\,\overline{ds} = -p\bar{\boldsymbol{n}}\,\overline{ds}, \tag{A.14}$$

where $\bar{\boldsymbol{T}}$ is the total Cauchy stress, $\bar{\boldsymbol{n}}$ is the total normal, $\overline{ds}$ is an area element in the perturbed configuration, p represents either p_{in} or p_{out}, depending on which boundary is under consideration, and we note that, from the static boundary conditions, we have

$$\boldsymbol{T}\boldsymbol{n}\,ds = -p\boldsymbol{n}\,ds, \tag{A.15}$$

where $\boldsymbol{n}$ is the outer unit normal to the boundary and ds is an area element in the statically deformed configuration.

Nanson's formula (**2**) for an incompressible material, applied to the incremental deformation gives

$$\bar{\boldsymbol{n}}\,\overline{ds} = \boldsymbol{f}^{-T}\boldsymbol{n}\,ds, \tag{A.16}$$

where $\boldsymbol{f} = \boldsymbol{I} + \boldsymbol{\gamma}$ is the deformation gradient tensor associated with the perturbation. Using (A.16) in (A.14), and subtracting (A.15), we obtain $\bar{\boldsymbol{T}}\boldsymbol{f}^{-T}\boldsymbol{n}\,ds - \boldsymbol{T}\boldsymbol{n}\,ds = -p\boldsymbol{f}^{-T}\boldsymbol{n}\,ds + p\boldsymbol{n}\,ds$, which, using $\bar{\mathbf{T}} = \mathbf{T} + \tau$, gives

$$(\boldsymbol{\tau}\boldsymbol{f}^{-T} + \boldsymbol{T}(\boldsymbol{f}^{-T} - \boldsymbol{I}))\boldsymbol{n} = p(\boldsymbol{I} - \boldsymbol{f}^{-T})\boldsymbol{n}, \tag{A.17}$$

where τ is the Cauchy stress associated with the perturbation. To derive an expression for τ in terms of known quantities, we note that, for an incompressible material,

$$\bar{\mathbf{T}} = \bar{\mathbf{F}}\bar{\mathbf{S}}, \tag{A.18}$$

and

$$\mathbf{T} = \mathbf{F}\mathbf{S}, \tag{A.19}$$

where $\bar{\mathbf{F}} = \mathbf{f}\mathbf{F}$ is the total deformation gradient tensor, $\bar{\mathbf{S}} = \mathbf{S} + \mathbf{s}$ is the total nominal stress tensor, and $\mathbf{S}$ is the nominal stress in the statically deformed configuration.

Now, (A.18) can be rewritten as

$$\mathbf{T} + \tau = (\mathbf{I} + \gamma)\mathbf{F}(\mathbf{S} + \mathbf{s}) = \mathbf{F}\mathbf{S} + \mathbf{F}\mathbf{s} + \gamma\mathbf{F}\mathbf{S} + O(|\mathbf{u}|^2), \tag{A.20}$$

hence, using (A.3) and (A.19), and neglecting $O(|\mathbf{u}|^2)$ terms, we have

$$\tau = \zeta + \gamma\mathbf{T}. \tag{A.21}$$

Now,

$$\boldsymbol{f}^{-T} - \boldsymbol{I} = \boldsymbol{I} - \boldsymbol{\gamma}^T - \boldsymbol{I} + O(|\boldsymbol{u}|^2) = -\boldsymbol{\gamma}^T + O(|\boldsymbol{u}|^2). \tag{A.22}$$

Hence, (A.17), to first order in $|\boldsymbol{u}|$, becomes

$$\boldsymbol{\tau}\boldsymbol{n} = \boldsymbol{T}\boldsymbol{\gamma}^T\boldsymbol{n} + p\boldsymbol{\gamma}^T\boldsymbol{n}. \tag{A.23}$$

Equation (A.23) simplifies to $q = 0$ and

$$v'(a) - \frac{v(a)}{a} = v'(b) - \frac{v(b)}{b} = 0. \tag{A.24}$$

We note that Engin and Şuhubi (**16**) decomposed the total normal as $\bar{\boldsymbol{n}} = \boldsymbol{n} + \boldsymbol{n}'$, where $\boldsymbol{n}'$ is a small vector associated with the perturbation, but instead of applying (A.14), they applied

$$\bar{\boldsymbol{T}}\bar{\boldsymbol{n}} = -p\boldsymbol{n}, \tag{A.25}$$

therefore, neglecting the contribution from the perturbation term $-p\boldsymbol{n}'$. This leads to erroneous results and means that their fundamental mode does not have a dispersion curve that passes through the origin. This is in contrast to results shown in Figs 8–10, and is inconsistent with the analytical results revealed in Section 3.2.

APPENDIX B

B. Elliptic integral representation of $\xi(\varrho)$

Consider the following indefinite integral representation of $\xi(r)$ as defined in Section 3.4,

$$\xi(r) = \int^r \sqrt{q(\varrho)}\, d\varrho = \int^r \frac{\sqrt{4\beta^2(\varrho^6 + a_2\varrho^4 + a_1\varrho^2 + a_0)}}{2\varrho(\varrho^2 + \alpha)}\, d\varrho, \tag{B.1}$$

with $a_2 = [4\alpha(\beta^2 + \delta) - 3]/(4\beta^2)$, $a_1 = 2\alpha(2\alpha\delta - 3)/(4\beta^2)$, $a_0 = \alpha^2/(4\beta^2)$ and noting that α, β^2 and δ are real with $\delta \geqslant 0$. If we make a change of integration variable via $z = \varrho^2$, (B.1) can be recast, after rationalizing the numerator, as

$$\int^r \sqrt{q(\varrho)}\, d\varrho = \frac{|\beta|}{2} \int^\zeta \frac{R(z)}{\sqrt{\Omega(z)}}\, dz \tag{B.2}$$

with $\zeta = r^2$ and with $R(z)$ and $\sqrt{\Omega(z)}$ defined as

$$R(z) = \frac{(z + z_1)(z + z_2)(z + z_3)}{z(z + \alpha)}, \quad \sqrt{\Omega(z)} = \sqrt{(z + z_1)(z + z_2)(z + z_3)}. \tag{B.3}$$

Here $-z_1$, $-z_2$ and $-z_3$ are the roots of the cubic equation with real coefficients, $\Omega(z) = z^3 + a_2z^2 + a_1z + a_0 = 0$. The integrand of (B.2) is a rational function of z and $\sqrt{\Omega(z)}$. For repeated roots of $\Omega(z)$, the integral can be expressed in terms of elementary functions. For non-repeated roots, it can be expressed in terms of three incomplete elliptic integrals as follows,

$$F(\phi|m) = \int_0^\phi \frac{d\theta}{\left(1 - m\,\sin^2\theta\right)^{1/2}}, \quad E(\phi|m) = \int_0^\phi \left(1 - m\,\sin^2\theta\right)^{1/2} d\theta,$$

$$\Pi(n;\phi|m) = \int_0^\phi \frac{d\theta}{\left(1 - n\,\sin^2\theta\right)\left(1 - m\,\sin^2\theta\right)^{1/2}}.$$

These Legendre integrals are known, respectively, as elliptic integrals of the first, second and third kinds. We shall use here elliptic integrals in the most general form, with ϕ defined as the real or complex amplitude, m the real or complex modulus and n the real or complex parameter. Additionally, we assume $1 - \sin^2\phi \in \mathbb{C}\backslash(-\infty, 0]$ and $1 - m\sin^2\phi \in \mathbb{C}\backslash(-\infty, 0]$, except that one of them may be 0 and $1 - n\sin^2\phi \in \mathbb{C}\backslash\{0\}$ (see §19.2(ii) of (**19**)).

Using polynomial long division and partial fraction expansion, we may rewrite $R(z)$ as

$$R(z) = \mathcal{C}_1 + z + \frac{\mathcal{C}_2}{z} + \frac{\mathcal{C}_3}{z+\alpha}, \tag{B.4}$$

with $\mathcal{C}_1 = E_1 - \alpha$, $\mathcal{C}_2 = E_3/\alpha$, $\mathcal{C}_3 = (\alpha^3 - E_1\,\alpha^2 + E_2\,\alpha - E_3)/\alpha$ and the so called elementary symmetric polynomials $E_1 = z_1 + z_2 + z_3$, $E_2 = z_1z_2 + z_1z_3 + z_2z_3$, and $E_3 = z_1z_2z_3$. Hence, $\xi(\zeta)$ can be expressed in four parts by

$$I_1(\zeta) = \frac{|\beta|}{2}\,\mathcal{C}_1 \int^{\zeta} \frac{1}{\sqrt{\Omega(z)}}\,dz, \quad I_2(\zeta) = \frac{|\beta|}{2} \int^{\zeta} \frac{z}{\sqrt{\Omega(z)}}\,dz,$$

$$I_3(\zeta) = \frac{|\beta|}{2}\,\mathcal{C}_2 \int^{\zeta} \frac{1}{z\sqrt{\Omega(z)}}\,dz, \quad I_4(\zeta) = \frac{|\beta|}{2}\,\mathcal{C}_3 \int^{\zeta} \frac{1}{(z+\alpha)\sqrt{\Omega(z)}}\,dz.$$

B.1 *Integration of* I_1

The cubic polynomial $\Omega(z)$ can be transformed into bi-quadratic form using the substitution $z = t^2 - z_1$. Traditionally z_1 is chosen as the real root, however this is not a restriction here, since we shall use elliptic integrals in their most general form (with complex arguments). Hence, defining $d = 1/\sqrt{z_3 - z_1}$, and after two additional transformations, $d^2t^2 + 1 = u^{-2}$ and $u = \sin\theta$, I_1 becomes

$$I_1 = \frac{|\beta|}{2}\,\mathcal{C}_1 \int^{\tau} \frac{2cd}{\sqrt{(1+c^2t^2)(1+d^2t^2)}}\,dt = -(2d)\,\frac{|\beta|}{2}\,\mathcal{C}_1 \int^{\upsilon} \frac{du}{\sqrt{1-m\,u^2}\sqrt{1-u^2}}$$

$$= -(2d)\,\frac{|\beta|}{2}\,\mathcal{C}_1 \int_0^{\phi} \frac{d\theta}{\sqrt{1-m\,\sin^2\theta}} = -(2d)\frac{|\beta|}{2}\,\mathcal{C}_1\,F(\phi|m),$$

where $I_1(\varrho)$ is expressed in terms of the real or complex modulus m and the real or complex amplitude ϕ defined hereafter as

$$m = 1 - \frac{d^2}{c^2}, \quad \phi = \arcsin\left\{\left[1 + d^2\left(\varrho^2 + z_1\right)\right]^{-\frac{1}{2}}\right\}, \tag{B.5}$$

with $c = 1/\sqrt{z_2 - z_1}$ and $d = 1/\sqrt{z_3 - z_1}$.

B.2 *Integration of* I_2

Using $z = t^2 - z_1$ we can write $I_2(\tau) = I_{21}(\tau) + I_{22}(\tau)$ with

$$I_{21} = \frac{|\beta|}{2} \int^{\tau} \frac{-2cd\,z_1}{\sqrt{(1+c^2t^2)(1+d^2t^2)}}\,dt, \quad I_{22} = \frac{|\beta|}{2} \int^{\tau} \frac{2cd\,t^2}{\sqrt{(1+c^2t^2)(1+d^2t^2)}}\,dt.$$

Hence I_{21} can be easily derived, following Section B.1, as

$$I_{21}(\varrho) = (2d\,z_1)\frac{|\beta|}{2}\,F(\phi|m). \tag{B.6}$$

The derivation of I_{22} is considerably more lengthy. Using $d^2t^2 + 1 = u^{-2}$ we may write

$$I_{22} = -\frac{|\beta|}{d}\left\{\int^{\upsilon} \frac{du}{u^2\sqrt{1-mu^2}\sqrt{1-u^2}} - \int^{\upsilon} \frac{du}{\sqrt{1-mu^2}\sqrt{1-u^2}}\right\}.$$

Using the following relations

$$\frac{d}{du}\left(\frac{\sqrt{1-mu^2}\sqrt{1-u^2}}{u}\right) = \frac{mu^2}{\sqrt{1-mu^2}\sqrt{1-u^2}} - \frac{1}{u^2\sqrt{1-mu^2}\sqrt{1-u^2}},$$

$$\int^{\upsilon} \frac{m\,u^2}{\sqrt{1-mu^2}\sqrt{1-u^2}}\,du = \int^{\upsilon} \frac{du}{\sqrt{1-mu^2}\sqrt{1-u^2}} - \int^{\upsilon} \frac{\sqrt{1-mu^2}}{\sqrt{1-u^2}}\,du,$$

$$\int^{\upsilon} \frac{\sqrt{1-mu^2}}{\sqrt{1-u^2}}\,du = \int_0^{\phi} \sqrt{1-m\sin^2\theta}\,d\theta = E(\phi|m)$$

to obtain I_{22}, we may finally express $I_2(\varrho)$ as

$$I_2 = \frac{|\beta|}{2}\left\{\frac{2}{d}\frac{\sqrt{1-m\sin^2\phi}\sqrt{1-\sin^2\phi}}{\sin\phi} + \frac{2}{d}E(\phi|m) + 2dz_1\,F(\phi|m)\right\}. \tag{B.7}$$

B.3 *Integration of I_3 and I_4*

Again employing $z = t^2 - z_1$ and $d^2t^2 + 1 = u^{-2}$, we may recast I_3 as

$$\begin{aligned} I_3 &= \frac{|\beta|}{2}\mathcal{C}_2\int^{\tau} \frac{2cd}{(t^2-z_1)\sqrt{(1+c^2t^2)(1+d^2t^2)}}\,dt \\ &= \frac{2d^3}{(z_1\,d^2+1)}\frac{|\beta|}{2}\mathcal{C}_2\int^{\upsilon} \frac{u^2}{(u^2-\nu^2)}\frac{1}{\sqrt{1-mu^2}\sqrt{1-u^2}}\,du, \end{aligned}$$

with $\nu^2 = 1/(z_1d^2+1)$. Rewriting $u^2/(u^2-\nu^2) = 1 + \nu^2/(u^2-\nu^2)$ and then setting $u = \sin\theta$ we obtain

$$\begin{aligned} I_3 &= \frac{2d^3}{(z_1d^2+1)}\frac{|\beta|}{2}\mathcal{C}_2\left\{\int^{\upsilon} \frac{du}{\sqrt{1-mu^2}\sqrt{1-u^2}} + \int^{\upsilon} \frac{\nu^2\,du}{(u^2-\nu^2)\sqrt{1-mu^2}\sqrt{1-u^2}}\right\} \\ &= \frac{2d^3}{(z_1d^2+1)}\frac{|\beta|}{2}\mathcal{C}_2\left\{\int_0^{\phi} \frac{d\theta}{\sqrt{1-m\sin^2\theta}} - \int_0^{\phi} \frac{d\theta}{\left(1-n_1\sin^2\theta\right)\sqrt{1-m\sin^2\theta}}\right\} \\ &= \frac{2d^3}{(z_1d^2+1)}\frac{|\beta|}{2}\mathcal{C}_2\left\{F(\phi|m) - \Pi(n_1;m|\phi)\right\}, \end{aligned}$$

with $n_1 = (z_1d^2+1)$. The derivation of I_4 is obtained following the same steps as in I_3, hence

$$I_4 = \frac{2d^3}{((z_1-\alpha)d^2+1)}\frac{|\beta|}{2}\mathcal{C}_3\left\{F(\phi|m) - \Pi(n_2;m|\phi)\right\}, \tag{B.8}$$

with $n_2 = ((z_1-\alpha)d^2+1)$.

Adding I_1, I_2, I_3 and I_4 we finally obtain an integral representation for the independent variable ξ in the LG transformation,

$$\xi(r) = \frac{|\beta|}{2}\left\{\frac{2}{d}\frac{\sqrt{1-m\sin^2\phi}\sqrt{1-\sin^2\phi}}{\sin\phi} + \frac{2}{d}E(\phi|m) + \mathcal{D}_1 F(\phi|m) + \mathcal{D}_2\,\Pi(n_1;\phi|m) + \mathcal{D}_3\,\Pi(n_2;\phi|m)\right\}, \tag{B.9}$$

with constants $\mathcal{D}_1$, $\mathcal{D}_2$ and $\mathcal{D}_3$ defined as

$$\mathcal{D}_1 = 2d\,(z_1 - \mathcal{C}_1) + \mathcal{C}_2\frac{2d^3}{n_1} + \mathcal{C}_3\frac{2b^3}{n_2}, \quad \mathcal{D}_2 = -\mathcal{C}_2\frac{2d^3}{n_1}, \quad \mathcal{D}_3 = -\mathcal{C}_3\frac{2d^3}{n_2}. \tag{B.10}$$